

# THE DISTRIBUTION OF SATELLITE GALAXIES IN A $\Lambda$ CDM UNIVERSE

Ingolfur Agustsson & Tereasa G. Brainerd

Boston University, Institute for Astrophysical Research, 725 Commonwealth Ave., Boston, MA 02215

Submitted to The Astrophysical Journal

## ABSTRACT

We investigate the distribution of luminous satellite galaxies with respect to the symmetry axes of isolated host galaxies in a  $\Lambda$ CDM universe. The selection of "host" and "satellite" samples based upon three somewhat different algorithms, all of which yield nearly identical results. In projection on the sky, the satellites are located preferentially close to the major axes of the host halos, resulting in a substantially flattened distribution of satellites. The flatness of the satellite distribution compares remarkably well with the flatness of the dark mass associated with the host galaxies. The degree to which the satellites are distributed anisotropically with respect to the major axes of the projected host halos is, however, grossly in excess of the degree to which satellites in the Sloan Digital Sky Survey (SDSS) are distributed anisotropically with respect to the major axes of the images of the host galaxies. This may be an indication that the mass and light of the SDSS hosts is not in perfect alignment on the sky. To investigate this we use a number of prescriptions in which the angular momentum vectors of the host galaxies are closely aligned with the principle axes of the surrounding dark mass in order to assign position angles to images of the hosts. When the distribution of the satellites is then computed with respect to the major axes of the images of the hosts, the anisotropy in the distribution of satellite galaxies is reduced significantly. In particular, when the angular momentum vectors of the hosts are aligned with the minor axes of the dark mass contained within radii of  $r_{200}$  or  $r_{100}$ , the anisotropy is reduced to a level that is comparable to the anisotropy shown by the SDSS satellites. The reduction in the anisotropy is due to a combination of the misalignment of mass and light for the host galaxies and the fact that the ellipticity of the image of a host galaxy is a rather poor indicator of the ellipticity of its projected halo. Lastly, the anisotropy in the distribution of the satellites persists to projected radii  $r_p \sim 500$  kpc and likely reflects preferential mass accretion along filaments.

Subject headings: dark matter | galaxies: fundamental parameters | galaxies: dwarf | galaxies: halos | galaxies: structure

## 1. INTRODUCTION

In the standard cold dark matter (CDM) paradigm, large, bright field galaxies are expected to reside within halos of dark matter whose virial radii extend to distances of order  $100h^{-1}$  kpc to  $200h^{-1}$  kpc and whose virial masses are of order  $10^{12}h^{-1}M_\odot$  (e.g., Navarro, Frenk & White 1995, 1996, 1997). Until very recently, though, direct observational constraints on the nature of the halos surrounding galaxies have not been tremendously strong. In particular, it has been difficult to determine whether or not the halos of observed galaxies are consistent with the halos expected in CDM universes.

In the past couple of years, however, a good deal of progress has been made on this issue and, for the most part, two independent probes of the large-scale halo potential are leading to the conclusion that, at least on scales of  $r \lesssim 50h^{-1}$  kpc, the halos of observed galaxies are consistent with the halos of numerical galaxies in CDM simulations. The most recent investigations of weak galaxy-galaxy lensing have concluded that the density profiles of field galaxies are consistent with the expectations for halos in CDM universes (i.e., the "Navarro, Frenk & White", NFW, profile). See, e.g., Guzik & Seljak (2002), Hoekstra, Yee & Gladders (2004) and Kleinheinrich et al. (2004). Work on the kinematics of satellite galaxies in orbit about host galaxies in the Sloan Digital Sky Survey (SDSS; Prada et al. 2002) and the Two De-

gree Field Galaxy Redshift Survey (2dFGRS; Brainerd 2004a) has shown that the velocity dispersion profiles of the satellite galaxies,  $\sigma_v(r_p)$ , are in excellent agreement with the predictions of CDM. For a complete discussion of recent weak lensing and dynamical results on the halos of field galaxies, see the review by Brainerd (2004b).

While galaxy-galaxy lensing and the kinematics of satellite galaxies currently seem to be leading towards similar constraints on the characteristic depths of the halo potentials, direct constraints on the shapes of galaxy halos are scarce (see, e.g., the review by Sackett 1999 and references therein). The popular NFW halo profile is most often cast in its spherically-averaged form (e.g., Navarro, Frenk & White 1995, 1996, 1997); however, the halos of galaxies in CDM universes are not strictly spherically-symmetric but are instead triaxial. A triaxial fit to the density profiles of CDM halos with principle axes  $a$ ,  $b$ ,  $c$  is given by

$$\rho(R) = \frac{\rho_c}{(R/R_0)(1 + R/R_0)^3} \quad (1)$$

where

$$R^2 = a^2 \frac{x^2}{c^2} + \frac{y^2}{b^2} + \frac{z^2}{a^2} \quad (2)$$

(Jing & Suto 2002) and  $\rho_c = 1$  for the NFW profile. Here the concentration parameter is  $c_e = R_e/R_0$  where  $R_e$  is defined such that for an ellipsoid with major axis length  $R_e$ , the mean interior density is  $\rho_e(z)/c_e$ , and

$e = 5 \text{ vir} (a^2/bc)^{0.75}$ . That is, while the most commonly used form of the halo density profile in CDM universes is the spherically symmetric NFW profile, in general the halos of galaxies in CDM universes are not spherically symmetric and, in projection on the sky, the median halo ellipticity is  $e_{\text{halo}} = 0.3$ . (On small scales,  $r \ll r_{200}$ , the effects of gas cooling will make the halos somewhat rounder than this, but on scales  $r \sim r_{200}$ , the shapes of the halos are not greatly affected by the baryons. See, e.g., Kazantzidis et al. 2004.) Interestingly, the galaxy-galaxy lensing signal observed by Hoekstra, Yee & Gladders (2004) prefers lens halos that are somewhat flattened (projected ellipticity of  $e_{\text{halo}} = 0.33^{+0.07}_{-0.09}$ ), which is in good agreement with the expectations for CDM.

As demonstrated by Hoekstra, Yee & Gladders (2002), galaxy-galaxy lensing is a promising probe of the shape of the lens halo potential. However, the observational result is somewhat controversial owing to the unknown contribution of external shear caused by structures larger than galaxies (i.e., the presence of a nearby group or cluster will cause the mass of a lens galaxy to appear flattened in the direction of the group or cluster on the sky). Further, in order to extract the lensing signal due to flattened halos, Hoekstra, Yee & Gladders (2004) had to make the simplifying assumption that the major axes of their lens galaxies would be perfectly aligned with the major axes of the projected halo mass distributions. While this assumption seems reasonable (assuming the lens galaxies are relaxed systems), it may not hold strictly true. Numerical work by Navarro, Abadi & Steinmetz (2004) on the formation of disk galaxies in CDM universes has shown that, in 3 dimensions, the angular momentum vector of the disk tends to align with the intermediate axes of the inertia tensor of the local large-scale structure at turnaround and, therefore, there may be a systematic offset between the major axis of the mass of the halo (as projected on the sky) and the major axis of the image equivalent ellipse of the galaxy.

In addition to weak lensing, another possible probe of the flattening of dark matter halos is the distribution of satellite galaxies with respect to the symmetry axes of isolated host galaxies. That is, an observed anisotropy in the distribution of satellite galaxies (i.e., a deviation from circular symmetry on the sky) could be an indicator of a flattened halo potential. The history of such investigations has, however, been frustratingly inconclusive. Investigations by Holmberg (1969), Zartsky et al. (1997) and Sales & Lambas (2004) seem to show that satellite galaxies have a preference for clustering nearby to the minor axes of their host galaxies. Similarly, the 11 brightest satellites of the Milky Way form a flattened structure that is oriented roughly perpendicular to the disk (e.g., Lynden-Bell 1982; Majewski 1994). Investigations by Hawley & Peebles (1975), Sharp et al. (1979) and McGillivray et al. (1982) suggest that any anisotropy in the distribution of satellite galaxies relative to their hosts is at most rather small, and perhaps nonexistent. More recently, Brainerd (2004c) found that the satellites of isolated host galaxies in the SDSS show a marked anisotropy in their distribution, with a strong preference for being clustered close to the major axis of the host galaxy. While this result is certainly controversial at present, it is not

unprecedented; using a much smaller sample Valtonen et al. (1978) also found a tendency for compact satellites to be aligned with the major axes of highly inclined disk galaxies.

The goal of our current investigation is to determine whether, when selected in a manner identical to that used to select isolated host galaxies and their satellites from large redshift surveys, the luminous satellites of host galaxies in a CDM model exhibit any marked anisotropy in their distribution relative to their hosts. To do this, we use the publicly available CDM GIF simulation (Kaumann et al. 1999), which provides both galaxy catalogs and mass particle catalogs. The selection of isolated host galaxies and their satellites from the GIF simulation is presented in §2. The distribution of the GIF satellites with respect to the major axes of the host galaxy halos (as projected on the sky) is computed in §3. The possibility of misalignments between the observed position angles of host galaxy images and the major axes of their projected halos is explored in §4. A discussion of our results and a comparison to recent related numerical studies is given in §5. Throughout the remainder of the paper we adopt a value for the Hubble parameter of  $H_0 = 70 \text{ km s}^{-1} \text{ Mpc}^{-1}$ .

## 2. HOSTS AND SATELLITES IN THE CDM GIF SIMULATION

The full suite of GIF simulations consists of  $N$ -body, adaptive  $P^3M$  simulations of various CDM universes that are combined with a semi-analytic prescription for galaxy formation (see, e.g., Kaumann et al. 1999). Galaxy, halo, and particle files can be downloaded from the GIF project website, <http://www.mpa-garching.mpg.de/GIF>, for a wide range of redshifts. Here we use only the present (epoch  $z = 0$ ) data for the CDM GIF simulation in which  $\Omega_0 = 0.3$  and  $\Omega_\Lambda = 0.7$ , the box length is  $201.7 \text{ Mpc}$  (comoving), the mass per particle is  $2 \times 10^{10} \text{ Mpc}$ , and the softening length is  $28.6 \text{ kpc}$ . Further, we use the galaxy catalog in which the magnitudes of the CDM GIF galaxies were measured in the SDSS band passes. Following Brainerd (2004a), who compared the velocity dispersion profiles of GIF satellites to those of satellites in the 2dFGRS, we assign magnitudes in the  $b_r$  band to the GIF galaxies using the photometric transformation given by Norberg et al. (2002)

$$b_r = g^0 + 0.155 + 0.152(g^0 - r^0); \quad (3)$$

For the cosmological parameters used in the CDM GIF simulation, the absolute magnitude of an  $L$  galaxy in the  $b_r$  band is  $M_{b_r} = -20.43 \pm 0.07$ .

Host and satellite galaxies are selected by rotating the simulation randomly and projecting the galaxy distribution along the line of sight. Results below are obtained from 100 random rotations of the simulation. Following Brainerd (2004c), three somewhat different methods are used to select isolated host galaxies and their satellites. In Sample 1, host galaxies must be at least 2.5 times brighter than any other galaxy that lies within a projected radius of  $r_p < 700 \text{ kpc}$  and a relative radial velocity difference of  $|\Delta v| < 1000 \text{ km s}^{-1}$ . Satellites of the host galaxies in Sample 1 must be at least 6.25 times fainter than their host, must be located within a projected radius of  $r_p < 500 \text{ kpc}$ , and the host-satellite ve-

locity difference must be  $|\Delta v| < 500 \text{ km s}^{-1}$ . In Sample 2, host galaxies must be at least twice as bright as any other galaxy that lies within a projected radius of  $r_p < 2.86 \text{ Mpc}$  and a relative velocity difference of  $|\Delta v| < 1000 \text{ km s}^{-1}$ . Satellites of the host galaxies in Sample 2 must be at least 4 times fainter than their host galaxy, must be located within a projected radius of  $r_p < 500 \text{ kpc}$ , and the host-satellite velocity difference must be  $|\Delta v| < 1000 \text{ km s}^{-1}$ . In Sample 3, host galaxies must be at least 8 times brighter than any other galaxy that lies within a projected radius of  $r_p < 500 \text{ kpc}$  and a relative radial velocity difference of  $|\Delta v| < 1000 \text{ km s}^{-1}$ . Further, host galaxies in Sample 3 must be at least twice as bright as any other galaxy that lies within a projected radius of  $r_p < 1 \text{ Mpc}$  and a relative radial velocity difference of  $|\Delta v| < 1000 \text{ km s}^{-1}$ . Satellites of the host galaxies in Sample 3 must be at least 8 times fainter than their host galaxy, must be located within a projected radius  $r_p < 500 \text{ kpc}$  and the host-satellite velocity difference must be  $|\Delta v| < 500 \text{ km s}^{-1}$ . These criteria are intended to select only very isolated host galaxies and their satellites, and it is worth noting that both the Milky Way and M 31 would be rejected as host galaxies.

In addition, we reject all host-satellite systems for which the sum total of the luminosity of the satellites exceeds the luminosity of the host. We also reject all host-satellite systems for which the number of satellites exceeds a total of 9. These criteria eliminate a small number of systems which are more likely to be representative of cluster environments rather than truly isolated host-satellite systems. Further, we restrict our analysis to hosts with luminosities in the range  $0.5L_{b_j} < L < 5L_{b_j}$  since Brainerd (2004a) found that outside this luminosity range the kinematics of the satellites in the CDM GIF simulation were not consistent with a virialized population. Lastly, since our goal is to determine the locations of the satellite galaxies with respect to the principle axes of the hosts, we restrict our analysis to host-satellite systems in which the halo of the host galaxy contains at least 100 particles within the virial radius (to insure a reasonable measure of the principle axes of the halo mass distribution) and the ellipticity of the halo of the host galaxy as projected on the sky is  $\epsilon_{\text{halo}} = 1 - b/a > 0.2$  (to insure that the major axis of the projected mass distribution is well-determined). After all of the selection criteria have been imposed we find that the different rotations of the simulation yield, on average, 1786 hosts and 5752 satellites in Sample 1, 317 hosts and 1208 satellites in Sample 2, and 949 hosts and 2865 satellites in Sample 3.

Following Navarro, Frenk & White (1995, 1996, 1997) we define the virial radius of the halo of a host galaxy to be  $r_{200}$ , the radius at which the mean interior mass density is equal to 200 times the critical mass density. The virial mass of the halo is then the mass contained within the spherical overdensity region of radius  $r_{200}$ ,  $M_{200} = M(r_{200})$ . Given that we restrict our analysis to halos with at least 100 particles within the virial radius, the minimum host galaxy halo mass is therefore  $2 \times 10^{12} M_\odot$ . The virial radii and centers of the host galaxy halos are computed in 3 dimensions via an iterative scheme in which the halo is initially centered on the coordinates of the host galaxy. In projection on the sky, the offset between the center of mass of the halo deter-

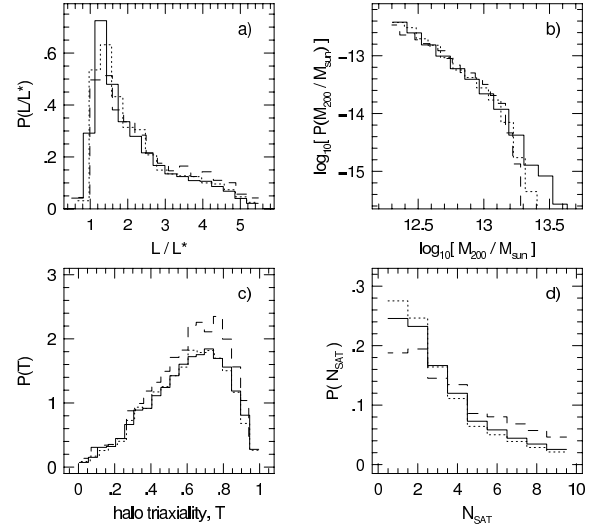


Fig. 1. | a) Probability distribution of host luminosities, b) Host halo mass function, c) Probability distribution of host halo triaxialities, d) Probability distribution for the number of satellites per host. In all panels the different line types correspond to the different host-satellite samples: Sample 1 (solid), Sample 2 (dashed), Sample 3 (dotted). See text for host and satellite selection criteria.

mined this way and the host galaxy is typically less than half a softening length.

All particles that are found within  $r_{200}$  for each host halo are used to compute the 3-dimensional shapes of the halos using a standard moment of inertia calculation that yields axis ratios  $b/a$  and  $c/a$  for each of the halos, where we define  $a \geq b \geq c$ . From the axis ratios, a triaxiality parameter is then computed for each of the host halos:

$$T = \frac{a^2 - b^2}{a^2 - c^2} \quad (4)$$

Here  $T = 0$  indicates a purely oblate object and  $T = 1$  indicates a purely prolate object.

Figure 1 shows the distribution of host luminosities, the mass function of the host halos, the distribution of host halo triaxiality parameters, and the distribution of the number of satellites per host in each of the three host-satellite samples. The median host luminosities are  $1.5L_{b_j}$ ,  $1.9L_{b_j}$  and  $1.8L_{b_j}$  for Samples 1, 2 and 3, respectively. The median virial mass of the host halos is  $3.5 \times 10^{12} M_\odot$ ,  $4.1 \times 10^{12} M_\odot$  and  $3.5 \times 10^{12} M_\odot$  for Samples 1, 2 and 3, respectively, and the median host halo triaxiality is  $T = 0.6$  for all three host-satellite samples.

### 3. DISTRIBUTION OF SATELLITES WITH RESPECT TO HOST MAJOR AXES

In her analysis of the distribution of satellite galaxies with respect to the symmetry axes of host galaxies in the SDSS, Brainerd (2004c) used the observed position angles of the images of the host galaxies to define the major axis of the light associated with the host galaxies. Assuming the host galaxies and their halos are relaxed, it is not unreasonable to expect that the major axis of the light emitted by a host galaxy should be fairly well aligned with the mass in the host galaxy's dark matter halo. Direct determinations of the degree of alignment of the symmetry axes of mass and light are difficult and rare, but in his study of strong lens galaxies, Kochanek (2002)

found that the major axes of the mass and light in the lens galaxies were aligned to within  $10^\circ$  in projection on the sky. Further, Hoekstra et al. (2004) found strong evidence for a flattening of the halos of weak galaxy lenses, under the a priori assumption that the major axis of the mass associated with the galaxy lenses was aligned with the major axes of the equivalent ellipses of the lens galaxy images.

The GIF simulation does not contain images of the simulated galaxies and, so, we cannot investigate the distribution of satellite galaxies with respect to actual images of host galaxies in the simulation. To begin our analysis of the distribution of satellite galaxies about their hosts, we use the principal moments of inertia of the host halos to construct full 3-dimensional ellipsoids that correspond to the distribution of mass particles found within the virial radii. For each rotation of the simulation, then, we compute 2-dimensional projections of the halo ellipsoids and use these to define the projected major and minor axes of the halos. Under the assumption that mass is aligned with light, then, we would expect that the major axes of the light emitted by the GIF hosts would be aligned with the major axes of the mass, as projected on the sky.

Shown in the left panels of Figure 2 are the differential probability distributions,  $P(\phi)$ , for the locations of the satellite galaxies, measured with respect to the major axes of the projected host galaxy halos. Here  $P(0^\circ)$  is the probability of finding a satellite whose location is perfectly aligned with the major axis of the projected halo mass and  $P(90^\circ)$  is the probability of finding a satellite whose location is perfectly aligned with the minor axis of the projected halo mass. From Figure 2, then, it is clear that the satellites in the GIF simulation are distributed anisotropically, with a strong preference for being aligned with the major axes of the projected halo mass. The degree of anisotropy in the satellite distribution is nearly identical for all three host/satellite samples.

Shown in the right panels of Figure 2 are the cumulative probability distributions,  $P(\phi \leq \phi_{\max})$ , for the locations of the satellites with respect to the major axes of the projected host halos (solid lines) as well as the cumulative probability for the locations of the actual particles in the halos (dashed line). From this figure, then, the distribution of satellites relative to the symmetry axes of the projected host halos is very similar to that of the particles in the halos. The satellites show a slightly flatter distribution than the particles, but overall the satellites trace the projected shapes of the halos rather well. We demonstrate this further in the top panel of Figure 3, where we show the median location of the satellites measured relative to the projected host halo major axis as a function of the ellipticity of the projected halo. The median location of the satellites in all three samples decreases approximately linearly with host halo ellipticity, although the slope is a bit steeper for the satellites than it is for the particles in the host halos. The satellite distribution in the top panel of Figure 3 is somewhat flatter than that of the particles in the host halos, but overall the flatness of the satellite distribution is a reasonable indicator of the flatness of the projected halos.

In her study of the distributions of SDSS satellite galaxies with respect to the major axes of host galaxies, Brainerd (2004c) found that the anisotropy of the

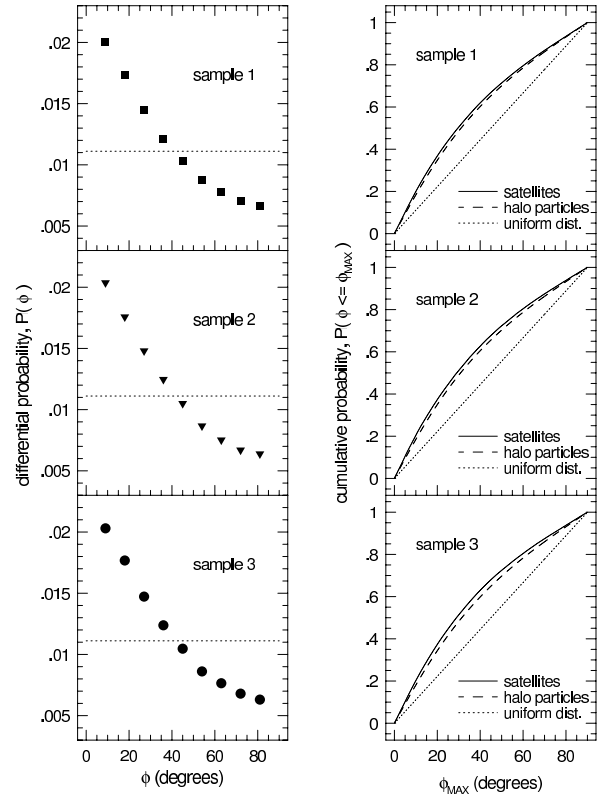


Fig. 2. Left panels: Differential probability distribution function for the location of satellites with respect to the major axes of the projected halo mass. Here  $\phi = 0^\circ$  corresponds to alignment with the projected halo major axis and  $\phi = 90^\circ$  corresponds to alignment with the projected halo minor axis. Dotted line shows the expectation for a uniform (circularly symmetric) distribution of satellites. Right panels: Cumulative probability distribution for the location of satellites (solid lines) and halo mass particles (dashed lines) with respect to the major axes of the projected halo mass. Top panels: Sample 1. Middle panels: Sample 2. Bottom panels: Sample 3. All satellites located within a projected radius of  $r_p < 500$  kpc have been used in the calculations.

satellite distribution occurs primarily on small scales ( $r_p \lesssim 100$  kpc) and that satellites with  $r_p \gtrsim 100$  kpc are distributed fairly isotropically. Brainerd (2004c) speculated that this could perhaps indicate that the virial region of the host halos extended to only about 100 kpc, with satellites at larger radii being part of an infalling population. We investigate this possibility in the bottom panel of Figure 3, where we show the median satellite location as a function of the satellite's projected radius, scaled by the virial radius of the halo (i.e.,  $r_p/r_{200}$ ). From this figure, then, the degree of anisotropy in the satellite distribution appears to be most pronounced for satellites with  $r_p \lesssim r_{200}$ , and the anisotropy persists to projected radii of order  $2r_{200}$ . This result compares rather poorly to the observation that the satellites of SDSS host galaxies seem to be distributed isotropically on large scales, and the resolution of this discrepancy is not at all obvious.

#### 4. MISALIGNMENT OF PROJECTED LIGHT AND MASS?

Although the sense of the anisotropy in the satellite distribution shown in Figure 2 is in good agreement with the observations of the SDSS galaxies found by Brainerd (2004c) (i.e., the satellites are found preferentially

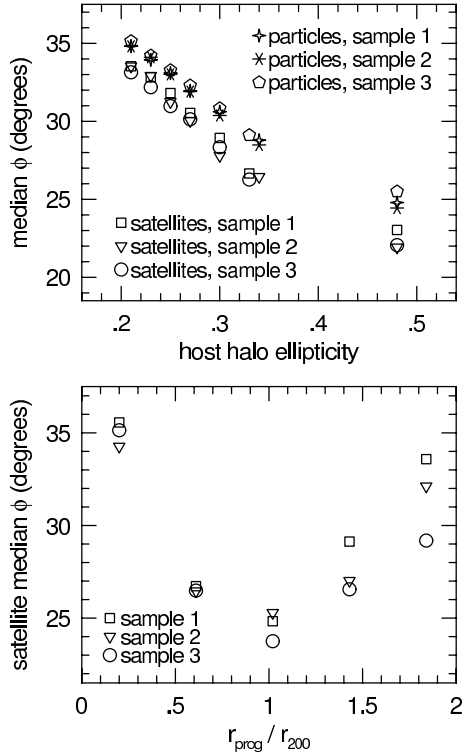


Fig. 3. Top panel: Median location of satellites and halo particles, measured with respect to the major axis of the projected host halo, as a function of the ellipticity of the projected halo. Here all satellites within  $r_p < 500$  kpc and all particles within  $r_{200}$  have been used in the calculation. Bottom panel: Median location of satellites as a function of projected radius on the sky, scaled in terms of the virial radius of the host galaxy halo. The median host halo virial radius is 275 kpc in all three samples. Here all hosts with projected ellipticity  $e_{\text{halo}} > 0.2$  have been used in the calculation. Bins have been chosen such that an equal number of objects falls within each bin.

close to the projected major axes of the host galaxies), the magnitude of the effect is grossly different. When measured relative to the major axis of the projected host halos, the median location of the G IF satellites is  $29^\circ$ . When measured relative to the major axes of the equivalent image ellipses of the host galaxies, the median location of the SDSS satellites is  $40.5^\circ$ . That is, if one assumes that the major axes of the images of the G IF host galaxies would be exactly aligned with the major axes of their projected halos, the G IF satellites are distributed much more anisotropically than are the SDSS satellites.

This could be an indication that the major axes of the images of the SDSS host galaxies are not perfectly aligned with the major axes of their projected halo masses. In addition, it is likely that the results in the previous section overestimate the degree of anisotropy that one would expect to find in an observed satellite distribution simply because in x2 we selected hosts on the basis of having a flattened mass distribution in projection on the sky. Recent numerical work by Libeskind et al. (2005) and Zentner et al. (2005) on the luminous satellites of Milky Way-type halos has shown that the satellites tend to lie in highly flattened structures that are essentially embedded in the principle planes of the host halos (i.e., the plane defined by the major and inter-

mediate moments of the inertia tensor). So, by choosing to use only host halos with substantial flattening in x2 we have likely introduced a selection effect that optimizes the degree to which the satellite population is observed to be flattened.

In an observational data set, of course, one cannot select host galaxies based upon an a priori knowledge of the flattening of their halos. Rather, what is commonly done is to select hosts on the basis of the ellipticity of their images. When searching for possible anisotropies in the distribution of satellite galaxies, hosts with particularly circular images are rejected from the sample for two reasons: (i) the position angle of the host is not well determined and (ii) it is expected that the latter is the image of the host, the latter will be the projected mass distribution of its halo on average. (See, e.g., Brainerd 2004c and Sales & Lambas 2004.)

In this section we therefore attempt to select host galaxies in the G IF simulation in a manner that is similar to what is done in large redshift surveys. In addition to the velocity difference and luminosity difference criteria outlined in x2, here we select host galaxies on the basis of the observed shape of a circular disk that is embedded in each of the host halos. The G IF simulation does not provide galaxy images, so it is not possible to do this on the basis of the G IF data alone. Rather, we make the simplifying assumption that all host galaxies are disk systems that are intrinsically circular. (While this is unlikely to be strictly true, a visual inspection of the 50 brightest host galaxies used by Brainerd 2004c shows them to be almost exclusively late-type disk systems.) The final observed ellipticity of the image of a host galaxy is then caused by a combination of the angle from which the simulation is viewed and how the host's disk is oriented with respect to its halo.

In order to place circular disks within the host halos we adopt three different criteria for the orientation of the disk angular momentum vectors,  $\vec{J}$ : (i) the angular momentum vector is aligned with the minor ("c") axis of the mass that is contained within a radius of  $r_{200}$ , (ii) the angular momentum vector is aligned with the minor ("c") axis of the mass that is contained within a radius of  $r_{100}$ , and (iii) the angular momentum vector is aligned with the intermediate ("b") axis of the mass that is contained within a radius of 2.5 Mpc. In the first case we are simply making the naive assumption that the disk lies in the principal plane of the virial mass. In the second case we are making the assumption that the disk lies in the principal plane defined by the mass contained within a sphere for which the density contrast is 100 times the critical density. While this second choice is not obvious, it is in good agreement with recent high-resolution numerical simulations of the formation of disk galaxies by Abadi et al. (2005). Our third choice for the orientation of the disks is motivated by work of Navarro, Abadi & Steinmetz (2004) on the formation of disk galaxies in CDM universes which showed that the angular momentum vectors of the disks tended to align with the intermediate axes of the inertia tensor of the local large-scale structure at turnaround. Here we use the inertia tensor of the local large-scale structure at the present epoch but, as Navarro, Abadi & Steinmetz (2004) note, the orientations of the principle axes of the inertia tensor

do not change substantially between turnaround and the present. Throughout, we will refer to our three methods of placing the disks within the host halos as  $J_{200}^C$ ,  $J_{100}^C$ , and  $J_{1ss}^b$ , respectively.

We repeat the host{satellite selection in the G IF simulation as before, but without regard to the shape of the projected halo in this case (i.e., round halos are explicitly allowed here). Following Brainerd (2004c), however, we restrict our analysis to the satellites of host galaxies for which the image of the projected disk is  $\epsilon_{\text{disk}} > 0.2$ . As in x2, we again require that all host galaxies have at least 100 particles within the virial radius,  $r_{200}$ , and we use 100 random rotations of the simulation in all cases below. Here the number of satellites and hosts in each of the samples is increased compared to x2 due to the fact that we now allow halos with  $\epsilon_{\text{halo}} > 0.2$ . The luminosity distributions, mass functions, and the distribution of the number of hosts per halo (e.g., Figure 1) are not, however, affected by the increased number of hosts and satellites. The mean number of hosts and satellites in a given rotation of the simulation is shown in Table 1 for each of our three different techniques for placing a circular disk at the location of the host galaxy.

Table 1: Mean Number of Hosts and Satellites

Sample	$N_{\text{hosts}}$	$N_{\text{sats}}$
Sample 1, $J_{200}^C$	2820	9393
Sample 2, $J_{200}^C$	479	1890
Sample 3, $J_{200}^C$	1506	4767
Sample 1, $J_{100}^C$	2824	9409
Sample 2, $J_{100}^C$	480	1897
Sample 3, $J_{100}^C$	1506	4766
Sample 1, $J_{1ss}^b$	2864	9522
Sample 2, $J_{1ss}^b$	516	2021
Sample 3, $J_{1ss}^b$	1558	4905

Here the major axis of a host galaxy's halo mass (i.e., the mass contained within the virial radius,  $r_{200}$ ) is not guaranteed to be aligned with the major axis of the host's projected circular disk. In x3 we simply assumed that the offset,  $\Delta\theta$ , between the major axis of the virial mass of the host galaxy and the major axis of its image would be zero. Shown in the left panels of Figure 4, however, are the actual probability distributions,  $P(\Delta\theta)$ , that we obtain when we place circular disks within the halos. The form of  $P(\Delta\theta)$  is essentially unaffected by the way in which the hosts and satellites are selected, but it is strongly affected by our choice of the orientation of the angular momentum vectors of the disks. In the case of the  $J_{200}^C$  hosts, the median value of  $\Delta\theta$  is 6.1° and one third of the hosts have values of  $\Delta\theta$  that exceed 11.4° (top left panel of Figure 4). For the  $J_{100}^C$  hosts the median value of  $\Delta\theta$  is 11.5° and one third of the hosts have values of  $\Delta\theta$  that exceed 18.8° (middle left panel of Figure 4). For the  $J_{1ss}^b$  hosts, the orientation of the projected disk major axis is almost completely uncorrelated with the orientation of the virial mass (bottom left panel of Figure 4); the median value of  $\Delta\theta$  is 43.3°, with one third of the hosts having a value of  $\Delta\theta$  that exceeds 58.9°.

Shown in the right panels of Figure 4 are the median

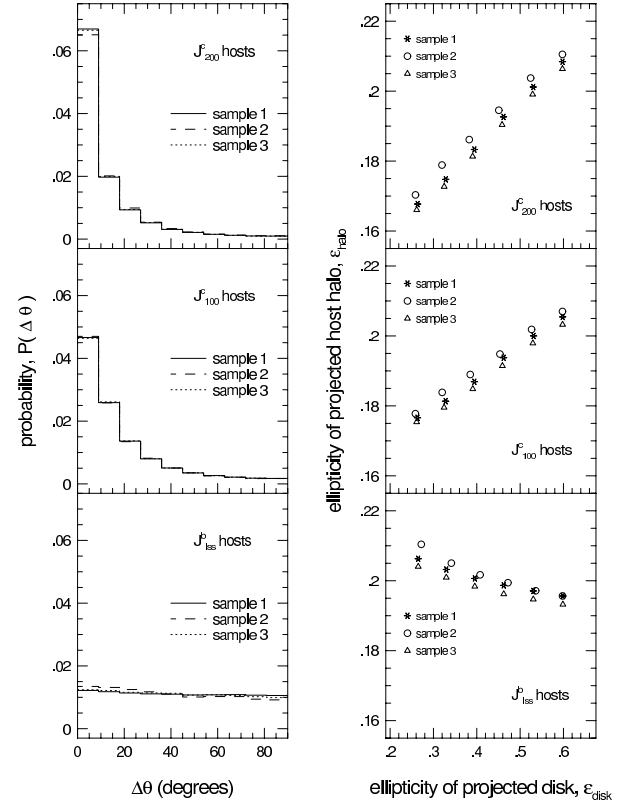


Fig. 4. Left panels: Probability distribution,  $P(\Delta\theta)$ , of the offset between the major axis of a host galaxy's projected halo mass (i.e., the mass contained within  $r_{200}$ ) and the major axis of the host's projected circular disk. Different line types indicate Sample 1 (solid lines), Sample 2 (dashed lines) and Sample 3 (dotted lines). Right panels: median ellipticity of the projected host halos as a function of the ellipticity of the projected disks. Different point types indicate Sample 1 (stars), Sample 2 (circles) and Sample 3 (triangles). Top panels:  $J_{200}^C$  hosts. Middle panels:  $J_{100}^C$  hosts. Bottom panels:  $J_{1ss}^b$  hosts. Host halos are defined to be all particles within  $r_{200}$ .

values of the projected ellipticity of the host halos,  $\epsilon_{\text{halo}}$ , as a function of the ellipticity of the projected circular disk,  $\epsilon_{\text{disk}}$ . Overall, there is a very weak dependence of the median value of  $\epsilon_{\text{halo}}$  on  $\epsilon_{\text{disk}}$ . In other words, the selection of hosts on the basis of a substantial flattening of their images is not equivalent to selecting hosts on the basis of a substantial flattening of their halos. For the  $J_{200}^C$  and  $J_{100}^C$  hosts the median value of  $\epsilon_{\text{halo}}$  increases with  $\epsilon_{\text{disk}}$ , but the trend is not at all dramatic. Linear extrapolations of the points in the top right and middle right panels of Figure 4 show that for the  $J_{200}^C$  and  $J_{100}^C$  hosts the median  $\epsilon_{\text{halo}}$  for truly edge-on disks is of order 0.25 while for truly face-on disks it is of order 0.14. Conversely, for the  $J_{1ss}^b$  hosts the median value of  $\epsilon_{\text{halo}}$  is a decreasing function of  $\epsilon_{\text{disk}}$ , leading to slightly rounder projected halos for edge-on disks and slightly flatter projected halos for face-on disks.

The reason for the trends in the right panels of Figure 4 is that the probability distributions of halo ellipticities,  $P(\epsilon_{\text{halo}})$ , change little as a function of the ellipticity of the projected disk. As an example of this, Figure 5 shows  $P(\epsilon_{\text{halo}})$  for different values of  $\epsilon_{\text{disk}}$  for the  $J_{200}^C$

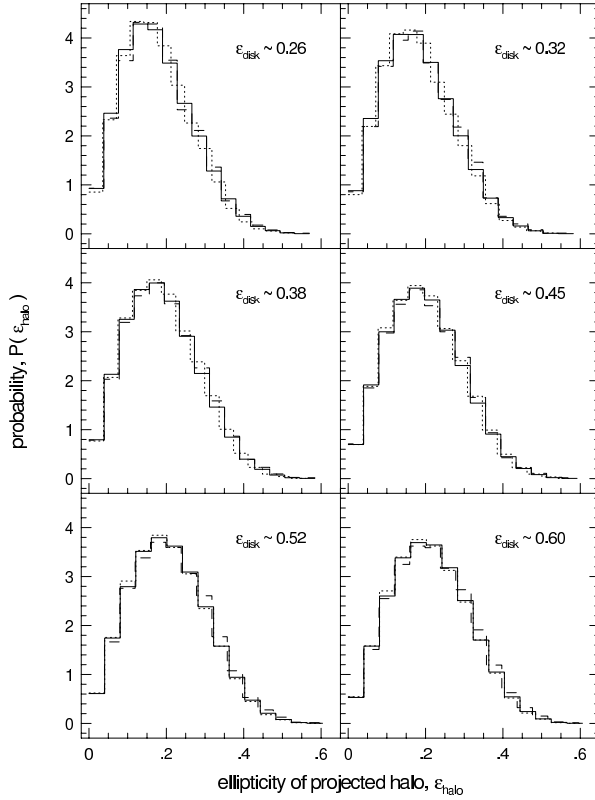


Fig. 5. | Probability distribution of the projected host halo ellipticity,  $P(\epsilon_{\text{halo}})$ , for  $J_{200}^C$  hosts with different projected disk ellipticities,  $\epsilon_{\text{disk}}$ . Different line types show Sample 1 (solid lines), Sample 2 (dashed lines) and Sample 3 (dotted lines). Host halos are defined to be all particles within  $r_{200}$ .

halos. Although  $P(\epsilon_{\text{halo}})$  changes from panel to panel in Figure 5, the changes are not dramatic and, therefore, selecting host galaxies on the basis of highly-elliptical images clearly does not preferentially select the very flattest halos, nor does it exclude the very roundest halos. This in mind, we expect that the distribution of the satellites of hosts that are selected on the basis of the flatness of their images (as opposed to the flatness of their halos) should be less anisotropic than the distribution found in x3 above.

Shown in Figure 6 are the differential and cumulative probability distribution functions,  $P(\epsilon)$  and  $P(\epsilon_{\text{max}})$ , for the locations of the satellite galaxies where is measured with respect to the major axis of the host's projected circular disk. The top panels show the results for Sample 1, the middle panels show the results for Sample 2, and the bottom panels show the results for Sample 3. Here all satellites found within  $r_p < 500$  kpc are used. Results for the different methods of placing disks within the host halos are indicated by the different point and line types (circles and dotted lines for  $J_{200}^C$  hosts, stars and dashed lines for  $J_{100}^C$  hosts, squares and solid lines for  $J_{100}^b$  hosts). Note that the panels of Figure 6 have the same scale as those in Figure 2 for direct comparison.

Figure 6 shows clearly that the degree to which the satellite galaxies are distributed anisotropically about the host galaxies is substantially reduced from the results shown in Figure 2. That is, when the satellite lo-

cations are measured with respect to the major axes of the projected host disks, a rounder distribution is seen than when the satellite locations are measured with respect to the major axes of the projected host halos. The degree to which the anisotropy in the satellite distribution is reduced does not depend strongly upon the way in which the hosts and satellites are selected, but there is a strong dependence on the way in which the host circular disk is placed within the halo. This is unsurprising given that the degree to which the misalignment between the major axis of the projected host disk and the major axis of the projected host halo depends upon the way in which the disk is placed within the halo. In the case of the  $J_{200}^C$  and  $J_{100}^C$  hosts, the median value of  $\epsilon$  is nearly identical: 35 and 35.5, respectively. In the case of the  $J_{100}^b$  hosts, the satellite distribution is close to being uniform (i.e., the anisotropy is almost completely destroyed), with a median satellite location of 44.

Again, as in x3, the sense of the anisotropy shown by the distribution of satellites about the  $J_{200}^C$  and  $J_{100}^C$  hosts is the same as that seen for the satellites of SDSS host galaxies; the satellites show a preference for being clustered close to the major axes of the images of the host galaxies. Like the results in x3, the G IF satellites are distributed more anisotropically than the SDSS satellites (a median value of 35 for the G IF satellites versus a median value of 40.5 for the SDSS satellites). However, here the degree of anisotropy of the distribution of satellites has been significantly reduced (i.e., the median value of  $\epsilon$  from x3 is 29). Also, as shown by the nearly complete lack of anisotropy in the distribution of the satellites of the  $J_{100}^b$  hosts, any random component that might cause the angular momentum vectors of the disks of the  $J_{200}^C$  and  $J_{100}^C$  hosts to be slightly misaligned with respect to the minor axis of the inertia tensor will only serve to decrease the anisotropy of the satellites. In particular, the results of Abadi et al. (2005) suggest that the angular momentum vectors of the host disks in our  $J_{100}^C$  analysis will be closely aligned with the minor axis only two thirds of the time. A combination of the facts that not all hosts will necessarily be disk galaxies, not all of hosts that are disk galaxies will have their angular momentum vectors precisely aligned in the manner that we adopted, and the positions angles of observed host galaxies are not known to within arbitrary accuracy, could easily account for the remaining discrepancy between the observed satellite distribution in the SDSS and the distribution of the G IF satellites for the  $J_{200}^C$  and  $J_{100}^C$  hosts. Conversely, the near lack of anisotropy in the satellites of the  $J_{100}^b$  hosts would suggest that if we do in fact live in a  $\Lambda$ CDM universe, the angular momentum vectors of the disks of the SDSS host galaxies are not particularly well-aligned with the intermediate axis of the local large-scale structure.

Shown in Figure 7 is the median satellite location,  $\epsilon$ , measured with respect to the major axes of the projected circular disks of the hosts. The open points in the left panels of Figure 7 show the dependence of  $\epsilon$  on the ellipticity of the host disk. All satellites within a projected radius of 500 kpc are used in the calculations for the left panels of this figure. In the case of the  $J_{200}^C$  and  $J_{100}^C$  hosts, the median value of  $\epsilon$  decreases with  $\epsilon_{\text{disk}}$

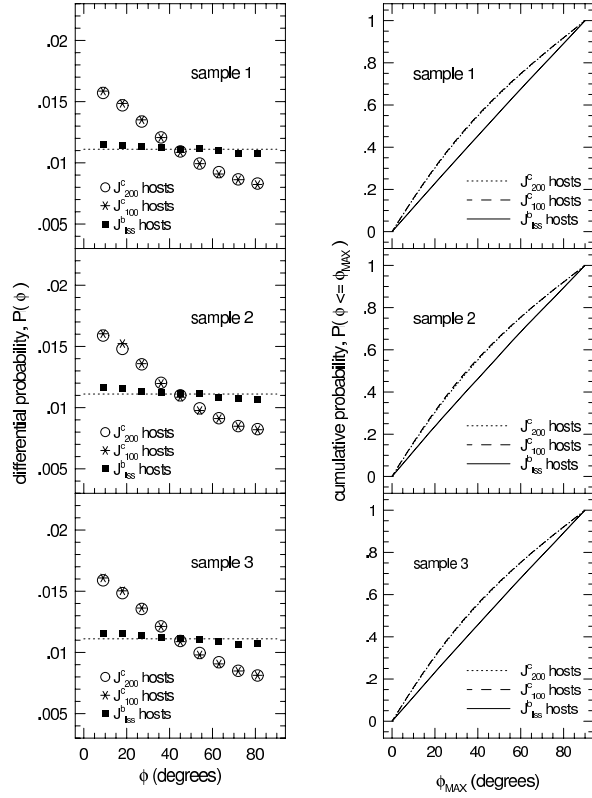


Fig. 6. | Probability distributions for the locations of satellite galaxies with respect to the major axes of the projected disks of their hosts. Hosts are required to have a projected ellipticity of  $\epsilon_{\text{disk}} > 0.2$ . Here all satellites within  $r_p < 500$  kpc are used. Top panels: Sample 1. Middle panels: Sample 2. Bottom panels: Sample 3. Left panels: Differential probability, where the dotted line indicates the expectation for a uniform distribution. Different point types show results for the  $J^C_{200}$  hosts (circles), the  $J^C_{100}$  hosts (stars), and the  $J^b_{100}$  hosts. Right panels: Cumulative probability. Different line types show Sample 1 (dotted line), Sample 2 (dashed line) and Sample 3 (solid line). In all panels the axis scales are identical to the corresponding panels in Figure 2 for comparison.

and, hence, the satellites of nearly edge-on hosts are distributed more anisotropically than those of nearly face-on hosts. For comparison, however, the crosses in the left panels of Figure 7 show the dependence of the median satellite location, measured with respect to the major axis of the projected halo, as a function of the ellipticity of the projected halo (i.e., the crosses are taken from the top panel of Figure 3). Clearly, the degree to which the satellites are seen to be distributed anisotropically depends much more strongly on shape of the projected halo than on the shape of the host galaxy's disk. This is, of course, simply a reflection of the fact that selecting hosts on the basis of a large in-plane ellipticity is not equivalent to selecting hosts on the basis of a large projected halo ellipticity (e.g., Figures 4 and 5).

In the case of the  $J^b_{100}$  hosts, the median satellite location is essentially independent of the ellipticity of the host disk (bottom left panel of Figure 7). This is simply a reflection of the fact that, in projection on the sky, the satellite galaxies track the projected mass distribution of the halo and, from Figure 4 (bottom left panel) the orientation of the disk for the  $J^b_{100}$  hosts is largely uncor-

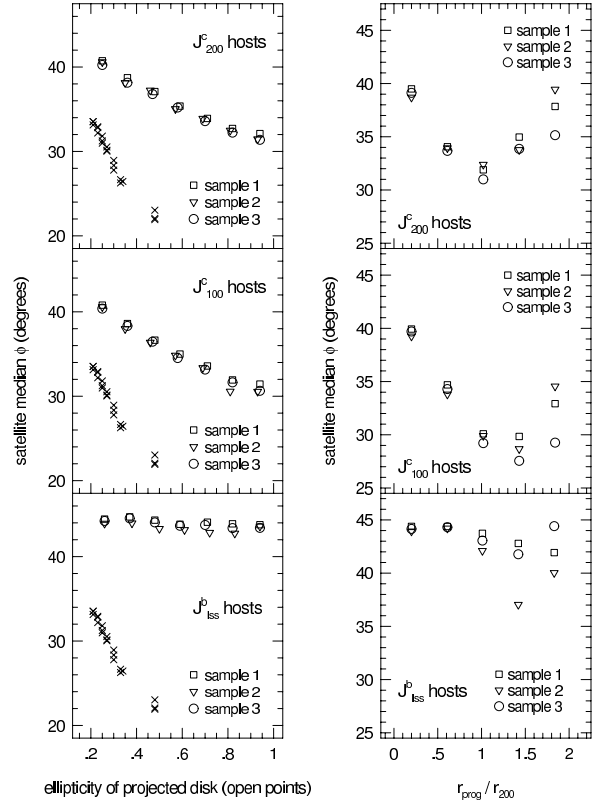


Fig. 7. | Left panels: Open points show the median satellite location, measured with respect to the major axis of the host galaxy's projected circular disk as a function of the ellipticity of the host's disk. Host disks are required to have  $\epsilon_{\text{disk}} > 0.2$ . Here all satellites within  $r_p < 500$  kpc have been used. For comparison, crosses show the median satellite location from the top panel of Figure 3 for all three samples as a function of the ellipticity of the projected host halo (i.e.,  $\epsilon$  is measured with respect to the major axis of the projected host halo). Right panels: Median satellite location, measured with respect to the major axis of the host galaxy's projected circular disk, as a function of projected radius,  $r_p$ . Here  $r_p$  is measured in units of the host galaxy's virial radius,  $r_{200}$ . Top panels:  $J^C_{200}$  hosts. Middle panels:  $J^C_{100}$  hosts. Bottom panels:  $J^b_{100}$  halos.

related with the orientation of the projected halo mass (i.e., the mass within  $r_{200}$ ).

The right panels of Figure 7 show the median satellite location, measured with respect to the major axis of the host disk, as a function of the projected radius. As in Figure 3, the projected radius has been scaled by the virial radius of the host halo. Again, the satellites of the  $J^b_{100}$  halos are distributed relatively isotropically over all scales. Like the satellites in Figure 3, however, the satellites of the  $J^C_{200}$  and  $J^C_{100}$  hosts show the greatest degree of anisotropy on scales of order 1 to 1.5 times the virial radius. That is, as in x3, the anisotropy in the distribution of the G I F satellites about their hosts remains significant on scales that are very much larger than that seen for the satellites of SDSS galaxies and, again, an explanation for this discrepancy is not immediately obvious.

## 5. DISCUSSION

We have shown that when isolated host galaxies and their satellites are selected from a CDM simulation in a manner that is identical to the way in which isolated host galaxies and their satellites are selected in large red-



shift surveys, the satellite galaxies in the simulation are distributed anisotropically about the symmetry axes of the projected mass distribution of the halos of the host galaxies. There is a strong preference for the satellite galaxies to trace out a flattened distribution on the sky, and the degree of flattening is strongly correlated with the flattening of the halos of the host galaxies. In projection on the sky, the distribution of the satellite galaxies relative to the major axes of the host halos is slightly flatter than the projected mass distribution of the halos themselves. When measured with respect to the major axes of the projected halos of the host galaxies, the shape of the satellite distribution is a reasonable indicator of the projected shapes of the host halos, being rounder for halos with low ellipticity and flatter for halos with high ellipticity and the median satellite location.

However, when measured with respect to the major axes of the projected host halos, the degree to which the G IF satellite galaxies are distributed anisotropically about their host galaxies far exceeds the degree of anisotropy shown by the satellites of SD SS host galaxies. Although the satellites of the SD SS host galaxies show a clear preference for being clustered close to the major axes of the images of the hosts, the SD SS satellites show a considerably less flattened distribution than do the G IF satellites under the assumption that the major axes of the projected halo mass distributions of the G IF hosts would be perfectly aligned with the major axes of the light emitted by the hosts.

Under the assumption that all of the G IF hosts are disk galaxies with angular momentum vectors aligned with various principle axes of the surrounding dark matter distribution, we find that the anisotropy shown by the G IF satellites is substantially decreased. Here the distribution of the satellites is measured relative to the major axes of the projected circular disks of the host galaxies and, on average, the major axes of the host disks are offset from the major axes of the projected halos. That is, the distribution of the satellites most strongly reflects the shape of the host halos, rather than the orientation of the host disks. When the host disks are aligned with the principle planes of the dark mass contained within radii of  $r_{200}$  and  $r_{100}$ , the offset between the symmetry axes of the mass and light of host galaxies is sufficiently small that the satellites exhibit a clear preference for being clustered close to the major axes of the images of the host galaxies. The anisotropy in the distribution of the G IF satellites is still, however, somewhat flatter than that of the SD SS satellites (median location of  $\sim 35^\circ$  for the G IF satellites and  $\sim 40.5^\circ$  for the SD SS satellites).

When the angular momentum vectors of the host disks are aligned with the intermediate axes of the local large-scale structure, there is little correspondence between the major axes of the projected host disks and the major axes of their projected halos. In this case, the anisotropy in the distribution of the G IF satellites about their hosts is almost completely erased (median location of  $\sim 44^\circ$ ), which demonstrates the importance of knowing how the images of host galaxies relate to their projected mass distributions if one wishes to perform robust tests of the predictions of CDM against observed host{satellite systems.

In all cases for which the G IF satellites are observed to show a marked tendency for clustering close to the ma-

for axes of the hosts (defined by either the halo mass or the image of the host), the anisotropy persists to very large physical scales ( $> 2r_{200}$ ). This likely reflects the tendency for structure in CDM universe to grow via non-spherical accretion (i.e., in simulations, mass particles and bound subhalos tend to be funneled into deep potential wells via filaments). The persistence of the anisotropy in the G IF satellite distribution at large physical radii is, however, somewhat of a puzzle in light of the fact that the satellites of SD SS host galaxies appear to be distributed quite isotropically on scales larger than

100 kpc. A resolution to this discrepancy is not obvious. However, it is important to keep in mind that the G IF and SD SS hosts are certainly not identical if for no other reason than the resolution limits of the simulation limit our analysis to rather massive isolated host galaxies. In addition, since there are no images of the hosts in the G IF simulation, we used very simple arguments based on precise alignments of the angular momentum vectors of the disks of the host galaxies with the surrounding mass distribution. Recent work by Abadi et al. (2005) suggests that only about two thirds of the G IF host disks should, in fact, be closely aligned with the minor axes of the inertia tensor associated with the mass inside  $r_{100}$ . Further, recent work by Bailin et al. (2005) on the formation of disk galaxies in CDM universes suggests that the orientation of the disk is aligned only with the inner halo and that the relative orientation of the inner and outer halo are essentially uncorrelated. All of these in combination could perhaps reconcile the lack of large-scale anisotropy in the distribution of SD SS satellite galaxies with the apparent large-scale anisotropy in the distribution of the G IF satellites.

Recently there have been a number of numerical investigations into the distribution of "satellites" residing within the halo of a host galaxy that is similar to the Milky Way (e.g., Kroupa, Thies & Boily (2005); Kang et al. 2005; Libeskind et al. 2005; Zentner et al. 2005). Kroupa et al. (2004) and Kang et al. (2005) relied on a priori assumptions that the distribution of satellites could be drawn simply from the distribution of dark matter particles and, so, their work is not particularly well-suited to direct comparison with ours. However, both Libeskind et al. (2005) and Zentner et al. (2005) used semi-analytic galaxy formation to select luminous satellites and, at some level, their results are directly comparable to ours.

There are a number of important differences between the Libeskind et al. (2005) and Zentner et al. (2005) investigations and the investigation presented here. First, both Libeskind et al. (2005) and Zentner et al. (2005) used simulations with much smaller volumes and much higher resolution order to address the apparent planar clustering of satellite galaxies in our own Milky Way. In their simulations Libeskind et al. (2005) and Zentner et al. (2005) were restricted to the study of only a small number of hosts (6 and 3, respectively), each of which had a large number of satellites, and the distribution of the satellites was computed independently for each host halo. Here we have used a large number of hosts with a wide range of masses and luminosities and, since most of our hosts have only a few satellites, our results for the distribution of the satellites is obtained by effectively "stacking" all of the host{satellite systems to-

gether. That is, the Libeskind et al. (2005) and Zentner et al. (2005) investigated what CDM predicts specifically for host galaxies that are like the Milky Way, while our study investigates what CDM predicts for large redshift surveys in which one is limited to only a few satellites per host galaxy.

Neither Libeskind et al. (2005) nor Zentner et al. (2005) selected host(satellite) systems in a way that mimics what is commonly done with large redshift surveys. Libeskind et al. (2005) combined semi-analytic galaxy formation with their N-body simulations and, so, there are truly luminous satellite galaxies (as opposed to simply "subhalos") present in the simulations. The satellites used by Libeskind et al. (2005) consist of the 11 most luminous satellites of each host galaxy, in analogy with the Milky Way system. Zentner et al. (2005) use two techniques to select satellites: semi-analytic galaxy formation and an association of satellites with the most massive surviving subhalos. Both Libeskind et al. (2005) and Zentner et al. (2005) conclude that the satellite populations of their Milky Way systems are strongly "attened" into thin, somewhat disk-like structures that are aligned with the longest principle axis of the dark matter halos of the host galaxies. They further conclude that, in the case of the Milky Way, the observed distribution of the satellites implies that the longest principle axis of the Milky Way's halo is oriented perpendicular to the disk. (It should be noted, however, that there are no actual luminous disks for the host galaxies in these simulations so neither study demonstrated directly that the disks of host galaxies are anti-aligned with the longest principle axes of the halos.)

Our work here agrees well with the sense of the anisotropy of the satellites found by Libeskind et al. (2005) and Zentner et al. (2005); the satellites are found

in an attenuated, rather than spherical, distribution and that distribution is well-aligned with the longest principle axis of the halo of the host galaxy. Because there are so few G I F satellites per host galaxy, however, we cannot address the question as to whether the satellites of any one host galaxy are typically found in an extremely attenuated, nearly-planar structure. Like the results of Libeskind et al. (2005) and Zentner et al. (2005), however, our results for the anisotropic distribution of the G I F satellites does seem to be a reflection of the fact that satellites are accreted preferentially along filaments.

Whether or not the distribution of satellite galaxies in CDM universes agrees with that of observed satellite galaxies in large redshift surveys remains an open question. Here we have shown that the sense of the observed anisotropy (a preference for clustering of satellites near to the major axes of the images of host galaxies) is consistent with the sense of the anisotropy that one would expect in a CDM universe, under the assumption that the major axes of the images of host galaxies are at least modestly correlated with the major axes of their projected halos. A proper resolution to the discrepancies that we find between observation and theory awaits simulations that are of considerably higher resolution and which address the details of the orientations of the visible hosts with respect to their dark matter halos.

#### ACKNOWLEDGMENTS

We are pleased to thank Mario Abadi, Brad Gibson, and Julio Navarro for discussing their current work with us in advance of its publication. Support under NSF contract AST-0406844 (IA, TGB) is gratefully acknowledged.

#### REFERENCES

- Abadi, M., Navarro, J. F. 2005, in preparation
- Bailin, J., Kawata, D., Gibson, B., Steinmetz, M., Navarro, J. F., Brook, C. B., Gill, S. P. D., Ibata, R. A., Lewis, G. F. & Okamoto, T. 2005, submitted to ApJ
- Bainard, T. G. 2004a, submitted to ApJ (astro-ph/0409381)
- Bainard, T. G. 2004b, in "The New Cosmology", AIP Conf. Proc. vol. 743, eds. R. E. Allen, D. V. Nanopoulos and C. N. Pope, 129 (astro-ph/0411244)
- Bainard, T. G. 2004c, submitted to ApJ (astro-ph/0408559)
- Guzik, J. & Seljak, U. 2002, MNRAS, 335, 311
- Hoekstra, H., Yee, H. K. C. & Gladders, M. D. 2004, ApJ, 606, 67
- Holmberg, E. 1969 Ark. Astron., 5, 305
- Jing, Y. P. & Suto, Y. 2002, ApJ, 574, 538
- Kang, X., Mao, S., Gao, L. & Jing, Y. P. 2005, submitted to A & A (astro-ph/0501333)
- Kaumann, G., Colberg, J. M., Diaferio, A. & White, S. D. M. 1999, MNRAS, 303, 188
- Kazantzidis, S., Kuvshinov, A. V., Zentner, A. R., Allgood, B., Nagai, D. & Moore, B. 2004, ApJ, 611, L2004
- Keinhehl, M., Schneider, P., Rix, H.-W., Erben, T., Wolf, C., Schirmer, M., Meisenheimer, K., Borch, A., Dye, S., Kovacs, Z., & Wisotzki, L. 2004, submitted to A & A (astro-ph/0412615)
- Kroupa, P., Thies, C. & Boily, C. M. 2005, A & A, 431, 517
- Kochanek, C. S. 2002, in proceedings of "The Shapes of Galaxies and their Halos", ed. P. Natarajan (World Scientific)
- Libeskind, N. I., Frenk, C. S., Cole, S., Helly, J. C., Jenkins, A., Navarro, J. F. & Power, C. 2005, submitted to MNRAS (astro-ph/0503400)
- Lynden-Bell, D. Obs., 102, 202
- McGillivray, H. T., Dodd et al. 1982, MNRAS, 198, 605
- Majewski, S. R. 1994, ApJ, 431, L17
- Navarro, J. F., Abadi, M. G. & Steinmetz, M. 2004, ApJ, 613, L41
- Navarro, J. F., Frenk, C. S. & White, S. D. M. 1995, MNRAS, 275, 720
- Navarro, J. F., Frenk, C. S. & White, S. D. M. 1996, ApJ, 462, 563
- Navarro, J. F., Frenk, C. S. & White, S. D. M. 1997, ApJ, 490, 493
- Notberg, P., Cole, S., Baugh, C. M., Frenk, C. S., Baldry, I., Bland-Hawthorn, J., Bridges, T., Cannon, R., Colless, M., et al. 2002, MNRAS, 336, 907
- Prada, F., Vitvitska, M., Klypin, A., Holtzman, J. A., Schlegel, D. J., Rebel, E., Rix, H.-W., Brinkmann, J., McKay, T. A. & Sabat, I. 2003, ApJ, 598, 260
- Sackett, P. D. 1999, in "Galaxy Dynamics", ASP Conf. Series 182, eds. D. R. Merritt, M. Valluri & J. A. Sellwood, 393
- Sales, L. & Lambas, D. G. 2004, MNRAS, 348, 1236
- Sharp, N. A., Lin, D. N. C. & White, S. D. M. 1979, MNRAS, 187, 287
- Valtonen, M., Teerikorpi, P. & Argyue, A. 1978, AJ, 83, 135
- Zaritsky, D., Smith, R., Frenk, C. & White, S. D. M. 1997, ApJ, 478, 39
- Zentner, A. R., Kuvshinov, A., Gnedin, O. Y. & Klypin, A. A. 2005, submitted to ApJ (astro-ph/0502496)